



## Research Papers

# How pressure affects costs of power conversion machinery in compressed air energy storage; Part I: Compressors and expanders

Zahra Baniamerian<sup>a,\*</sup>, Seamus Garvey<sup>a</sup>, James Rouse<sup>a</sup>, Bruno Cárdenas<sup>a</sup>, Daniel L. Pottie<sup>b</sup>, Edward R. Barbour<sup>b</sup>, Audrius Bagdanavicius<sup>c</sup>

<sup>a</sup> Mechanical and Aerospace Systems Research Group, University of Nottingham, Nottingham NG7 2TU, UK

<sup>b</sup> Centre for Renewable Energy System Technology (CREST), Loughborough University, Loughborough LE11 3TU, UK

<sup>c</sup> School of Engineering, University of Leicester, Leicester LE1 7RH, UK



## ARTICLE INFO

## Keywords:

Compressed air energy storage  
Power conversion system  
Cost per kW  
Storage pressure  
Compressor  
Expander

## ABSTRACT

This study addresses a critical economic aspect in compressed air energy storage that has not been discussed much in existing literature: the impact of operating pressure on machinery capital costs. It aims to answer whether the cost per unit of power for power conversion systems changes with the maximum storage pressure. Considering that higher storage pressures are associated with greater energy density, enhanced energy storage capabilities and improved system efficiency. This paper helps clarify uncertainties in initial cost estimations for power-generation plants. Effects of operating pressure on the components and overall sizes and consequently costs of power conversion machinery are individually investigated in two parts. Part I encompasses the compressor and expanders, and part II comprehensively discusses the effects of the operating pressure on the costs of heat exchangers. The analysis employs a conceptual engineering approach, revealing that higher intake pressure reduces overall compressor/expander size, leading to cost savings. Additionally, increasing the number of compression stages for higher storage pressures enhances exergy storage cost-effectiveness. To establish an advanced adiabatic CAES plant with a storage pressure of 200 bar instead of 50 bar, there is potential for a 6 % reduction in \$/kW expenditure.

## 1. Introduction

Compressed Air Energy Storage (CAES) is one of the most welcomed technologies for storing large quantities of electrical energy in the form of high-pressure air stored in vessels or caverns. CAES can provide several hours of plant-level scale output with attractive capital costs in comparison with other similar energy storage systems like emerging batteries for which the typical system capacities and storage sizes are an order of magnitude smaller than CAES (~10 MW, <10h) with significantly higher capital costs [1].

The capital expenditure for establishing a CAES system spans a wide range; 400–1000 \$/kW for conventional CAES, 850–1870 \$/kW for large scale adiabatic CAES, and 517–1550 \$/kW for small scale CAES [1].

There is some limited research investigating the economic aspects of advanced adiabatic CAES (AA-CAES) systems. However, most of these studies tend to focus on specific cases [1–11] or on combination of CAES with other technologies [2,12–14]. Adding an engineering conceptual

analysis in a general perspective is of great worth in this area. The following section reviews some of the most pertinent studies.

Cheyb et al. [1] analysed the cost of a small-scale trigenerative CAES (T-CAES) plant and compared it to electrochemical batteries. They found air storage vessels to be the most expensive component, with storage pressure impacting capital expenditure. In their study, as the energy scale grows up from 1 kWh to 2.7 MWh, CAES plant cost decreased from 90 USD/kWh.year to 30 USD/kWh.year. Importantly, they found T-CAES investment costs competitive with electrochemical batteries for long-duration storage.

Bushehri et al. [2] conducted an economic analysis of an innovative system integrating a green CAES, Organic Rankine Cycle (ORC), and Reverse Osmosis (RO) desalination unit. The system is designed to meet the power requirements of coastal cities, offering peak shaving, potable water, and domestic hot water. The proposed system demonstrates the capability to generate 37.48 MWh of electricity during 5 h of peak consumption and supply 349.56 m<sup>3</sup> of potable water daily. The estimated capital cost is approximately \$0.2 million per MWh.

Bazdar et al. [3] introduced a decentralized system for implementing

\* Corresponding author.

E-mail address: [zahra.baniamerian@nottingham.ac.uk](mailto:zahra.baniamerian@nottingham.ac.uk) (Z. Baniamerian).

Nomenclature	
$c_{blade}$	blade chord (m)
$C_x$	axial velocity in the compressor (m/s)
$D$	rotor diameter (m)
$D_h$	hub diameter (m)
$D_M$	mean diameter of compressors (m)
$D_s$	specific diameter
$D_t$	compressor rotor diameter (m)
$E_{kin,blade}$	kinetic energy of the blades (J)
$EX$	exergy
$g$	gravitational acceleration ( $m/s^2$ )
$h_{blade}$	blade height (m)
$H$	adiabatic head (m)
$J$	joint efficiency factor
$k$	heat capacity ratio
$L_C$	casing length, m
$m_{blade}$	blade mass (kg)
$\dot{m}_{air}$	air mass flowrate (kg/s)
$N$	rotational speed of the rotor (rpm)
$N_s$	specific speed
$N_{st}$	number of stages, within the casing of a compressor
$p$	pressure, bar
$p_0$	ambient pressure (Pa, bar)
$Q$	volume flow rate ( $m^3/s$ )
$\dot{Q}_{in}$	intake volume flow rate ( $m^3/s$ )
$r_c$	compression ratio
$S$	maximum allowable stress (MPa)
$t$	minimum required thickness
$T$	temperature ( $^{\circ}C$ , K)
$T_{ref}$	reference temperature (K)
$U_t$	tip velocity (m/s)
$V$	storage volume ( $m^3$ )
$W$	weight (kg)
CAES	compressed air energy storage
PCS	power conversion system
<i>Greek symbols</i>	
$\beta$	blade aspect ratio
$\eta$	efficiency
$\rho$	density ( $kg/m^3$ )
$\Pi$	ratio of the intake pressure of device B to device A
$\sigma_y$	yield stress (MPa)
$\varphi$	flow track angle

A-CAES within urban building infrastructure. The investigation encompasses various energy management operation strategies (EMOS), placing particular emphasis on decentralized A-CAES applications and focusing on the efficient management of surplus solar PV power. The paper revealed that the exclusive adoption of A-CAES for renewable integration with a Levelized Cost of Electricity (LCOE) of 0.110 \$/kWh is not economically viable, compared to the grid's 0.105 \$/kWh. Nonetheless, scenarios that involve utilizing surplus PV power for alternative purposes exhibit promise, leading to a reduction in LCOE by up to 5.7 %. According to the analysis, strategically planning A-CAES for load-shifting alongside solar energy integration ends up with LCOE of 0.090 \$/kWh.

Cao et al. [4] address the limitations of traditional ACAES, characterized by low turbine efficiency and power output due to insufficient heat recovery by proposing a combined cycle power system integrating CAES and high-temperature thermal energy storage. Energy, exergy, and economic (3E) analyses are conducted, revealing that, under design conditions, the system achieves an energy storage density of 5.77 kWh/ $m^3$ , LCOE of 0.1186 \$/kWh, and a dynamic payback period of 6.51 years.

Mersch et al. [5], employ a comprehensive thermo-economic optimization framework to evaluate various compressed-air energy storage configurations across different scales, with a specific focus on thermal energy stores, exploring both solid packed-bed and liquid options. The most promising configuration involves two packed-bed thermal energy stores using Basalt as the storage material, achieving an energy capital cost of 140 \$/kWh, a power capital cost of 970 \$/kW at a nominal discharge power of 50 MW with a 6-h charging/discharging duration. Solar salt emerges as the best-performing liquid storage material, with an energy capital cost of 170 \$/kWh and a power capital cost of 1230 \$/kW.

Zhao et al., proposed an energy, exergy, economic and environmental analyses for an AA-CAES system integrated with wind power. They found that a hybrid energy storage system based on A-CAES system and flywheel energy storage system, has excellent performance on smoothing out the fluctuations of wind power in comparison with independent energy storage system [7].

Matos et al. [8] presented various business models for assessing the economic viability of CAES for storing excess renewable energy sources (RES) and for energy arbitrage. They discovered that the CAES+RES

model outperformed the CAES arbitrage model. Moreover, they concluded that CAES is a feasible and profitable solution for RES energy storage, aiding in managing variability, reducing weather dependence, and enhancing grid integration. CAES did not fare well in the context of grid energy arbitrage in their study.

Madlener and Latz [9] evaluated the economic viability of using CAES to enhance wind power integration. They examined a wind park with 100 MW capacity in two scenarios: one with a separate central CAES plant and another with individual compressors on each wind turbine (without generators). Their findings favoured the centralized CAES plant.

Bozzolani [10], compared two existing energy storage technologies: Pumped Hydro Energy Storage (PHES) and adiabatic CAES (A-CAES) from the technical and economic points of view. They found that A-CAES has almost similar profitability as PHES with specific costs between 1000 and 1250 \$/kW. Bozzolani believed that although some very low-capital-cost cases have been reported (e.g., 350 \$/kW for the existing Guangzhou PHES), there is more evidence for costs consistent with 2000 \$/kW (Kazunogowa PHES) with only 75 % efficiency. This makes CAES plants appear more economically attractive than PHES.

Zakeri and Syri [11] performed a techno-economic comparison between the various energy storage technologies. The CAES system in their assessment has average capital cost of 812–960 \$/kW for above-ground installation and 1350–1460 \$/kW for underground installation.

Apart from the storage vessel, the primary cost components involved in establishing any type of CAES plant are associated with the PCS. For above-ground CAES plants, the cost of PCS constitutes around 90 % of the total expenses. However, for underground installations, PCS costs account for 98 % of the total expenses [11].

In existing literature, one significant economic aspect in power plants with a power conversion system (PCS) has remained unexplored: the influence of pressure on machinery capital costs, with a specific emphasis on CAES. A notable gap in the literature pertains to addressing the question: Does the cost per unit of power for the PCS machinery change with varying storage pressures? Significantly, all costs mentioned in the literature overlook the potential effects of operating pressure on machinery expenses. Addressing this question could provide valuable insights into the complexities of estimating initial costs for establishing a power generation plant and will suggest how future CAES plants should be designed such that any benefits can be exploited.

This study aims to fill this gap by assessing the engineering rationale linking PCS cost per power to operating pressure. In other words, this study investigates how operating pressure affects the size and cost of PCS turbomachinery. It aims to understand the size differences between machines designed for higher versus lower pressures and then derive the corresponding cost variations. In this regard, different storage pressures for AA-CAES plants are compared to examine how storage pressure impacts the overall cost.

## 2. Methodology

To assess the effects of pressure on the size and cost of PCS machinery, the AA-CAES application has been considered. In this section, an introduction to the AA-CAES system is provided to demonstrate how the number of PCS machinery components involved in the AA-CAES plant may be altered with an increase in pressure. In the subsequent section, the effects of operating pressure are examined by comparing PCS machinery within different stages.

Fig. 1 shows a schematic of a typical AA-CAES system. During periods of low-power demand, surplus electricity drives the reversible motor-generator units to run a chain of compressors for injecting air into a storage vessel or cavern. After each compression stage, the air is cooled to both enhance the compression efficiency and control thermal loads within the storage containment. The heat generated through the compression process is stored in a thermal storage unit (TES). When power generation fails to meet demand, the stored compressed air is released and heated using heat derived from the compression process (AA-CAES). Ultimately, the energy from the compressed air is harnessed by turbines.

This study examines storage pressures ranging from 10 to 350 bar, considering practical limits on compressor temperature. To prevent accelerated degradation due to damaging stresses in compressor blades, the air temperature within the compressor should not exceed 150 °C [15].

The compression of a gas is always associated with an increase in temperature. The extent of this increase depends on the nature of the process—whether it is isothermal, adiabatic, or isentropic. A polytropic process is characterized by a constant  $pV^n$ , where  $n$  is 1 for isotherm process and  $k$  for the adiabatic/isentropic processes. Based on this, it can be shown that the temperature increase associated with each compression stage, with a compression ratio denoted as  $r_c = \frac{p_2}{p_1}$  can be calculated by:

$$\frac{T_2}{T_1} = \left(\frac{p_2}{p_1}\right)^{\frac{n}{n-1}} \quad (1)$$

By assuming the compressors to be isentropic,<sup>1</sup>  $n = k$ , where  $k$  represents the heat capacity ratio of the air.

Preventing excessive temperatures in compressors is vital for improving longevity, efficiency, and safety. Elevated temperatures accelerate wear, degrade lubricants, and compromise materials. To regulate air temperature within compressors, those with higher compression ratios typically incorporate intercooling systems. However, in AA-CAES applications aimed at storing heat, it is more rational to select a lower compression ratio to eliminate the need for intercooling within the compressor. Instead, aftercooling is performed after each compressor stage to harness heat from the compression process.

To achieve a design with a maximum storage pressure of 350 bar—upper range of present study—and avoid exceeding 150 °C at each compression unit, a compression ratio of 2.42 has been selected. This

<sup>1</sup> It should be emphasized that this assumption is made solely to obtain a preliminary value for the compression ratio. Importantly, this simplification does not exert any influence on the primary calculations related to the paper's main objective.

value ensures that the outlet air temperature from the compressors never exceeds 100 °C, enabling the utilization of non-pressurized—a simple and cost-effective method of cooling—for heat storage (Fig. 2). This figure shows a 4-stage compression expansion plant which can provide maximum storage pressure of 34.3 bar. In the proposed plan the air intake temperature to each compressor stage is assumed to be equal to the ambient temperature (17 °C) and the emerging air temperature would be 100 °C.

Utilizing compressors with a maximum compression ratio of  $r_c = 2.42$ , achieving various storage pressures within the range of 10–350 bar requires distinct number of stages,  $n$ . (e.g. to achieve the storage pressure “ $p$ ,” the initial  $(n - 1)$  compressors would maintain a uniform compression ratio of 2.42, while the final stage compressor possess a compression ratio of  $\frac{p}{2.42^{(n-1)}}$ ). The number of compression stages for different storage pressures are presented in Table 1.

Using Eq. 1, by assuming the air as an ideal gas, the air temperature emerging from each of  $(n - 1)$  compressors would be equal to 100 °C. For each compression stage, a dedicated heat exchanger is devised to reduce the air's temperature from 100 °C to 17 °C before it enters the next compression stage; thereby ensuring the subsequent compression does not result in excessive system temperature. The utilization of the ideal gas assumption facilitates the uniformity of compressors and heat exchangers across all stages, differing solely in terms of air intake pressure.

After going through the compressor chain, the air is stored in a storage vessel/cavern maintaining at ambient temperature. The pressure exergy within the air storage containment,  $EX|_p$ , can be calculated by:

$$EX|_p = p_0 V (r \ln(r) - (r - 1)) \quad (2)$$

where,  $r$  represents the ratio of the storage pressure to the ambient pressure. The first term in this equation represents the work component due to the pressure difference when the compressed air expands from the high-pressure state to the initial ambient pressure. The second part, on the other hand, represents the flow component exergy associated with the change in pressure from ambient conditions to the compressed state.

The main objective is to explore how the size and cost of machinery vary against operating pressure as proceeding through the compression stages. This includes similar compressors, similar expanders, and then similar heat exchangers in Part II.

## 3. Effects of pressure on size and performance of PCS

Based on available reports on CAES plant costs, PCS machinery costs vary with storage pressure. Operating pressure significantly impacts machinery expenses. This analysis solely examines PCS machinery capital expenditure and its pressure-related impact, treating compressors and expanders similarly in pressure-performance/size analysis.

Turbines or compressors that need to operate across a range of power levels or deal with changing exhaust or intake pressures can be designed to perform well in a variety of conditions. This implies that multiple turbines/compressors with different geometries may be engineered to deliver similar performance characteristics. In this regard, the use of dimensionless numbers becomes instrumental in selecting performance parameters such as speed or rotor diameter during turbomachine design or when making comparisons between different machines.

Two dimensionless parameters are commonly used to describe compressors: specific speed  $N_s$ , and specific diameter  $D_s$ . These serve as convenient parameters for presenting the performance criteria as well as for comparing the performance of turbomachines [16]:

$$N_s = \frac{NQ^{0.5}}{(gH)^{0.75}} \quad (3)$$

$$D_s = \frac{D(gH)^{0.25}}{(Q)^{0.5}} \quad (4)$$

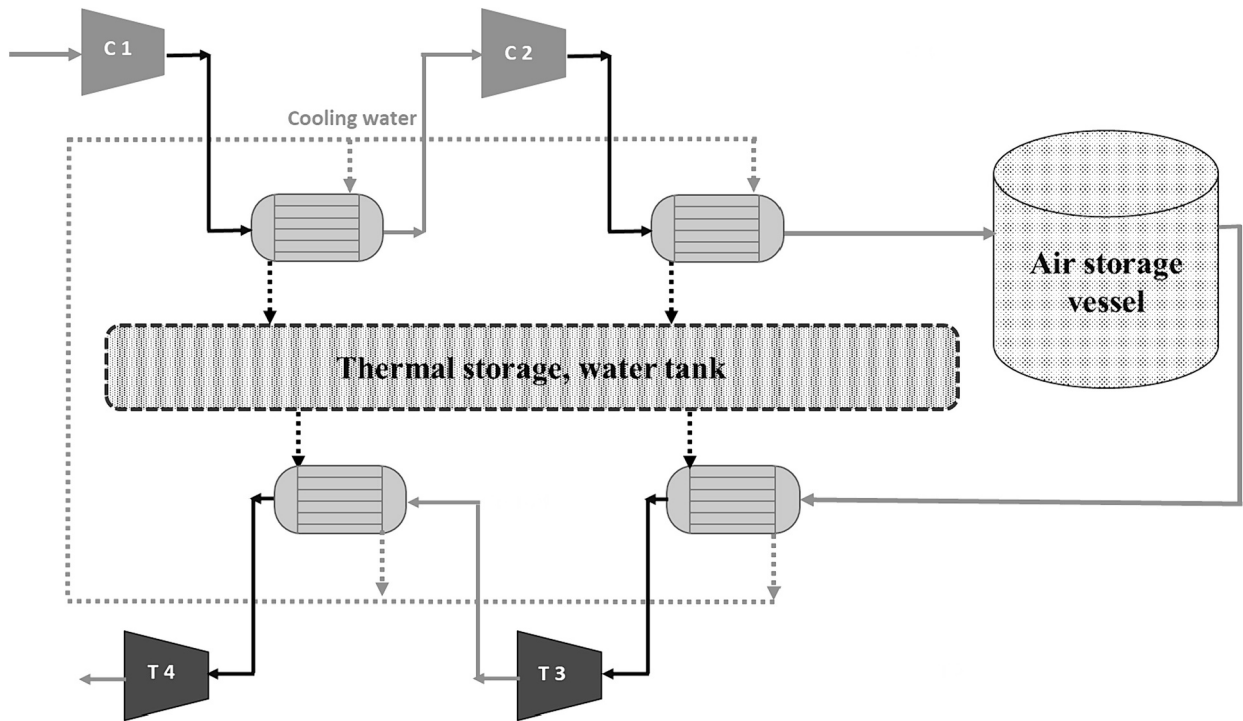


Fig. 1. Schematic of an AA-CAES system.

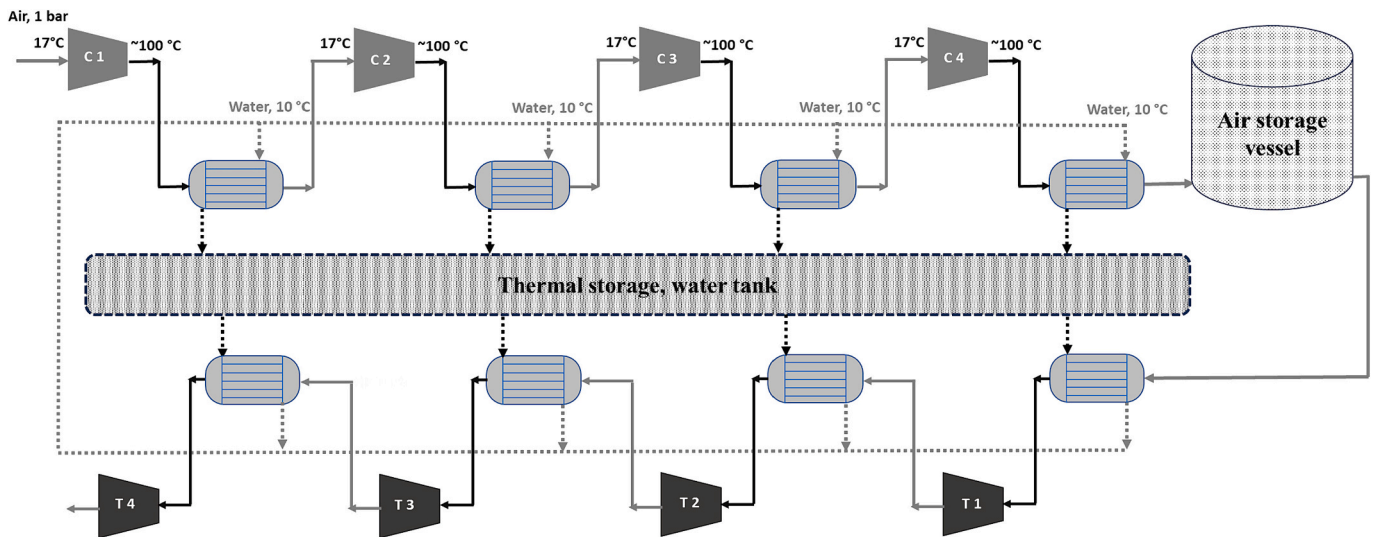


Fig. 2. Inlet and outlet temperature and pressure in a 4 stage-compression-expansion unit. The air and water temperatures are chosen in accordance with UK climate conditions.

For each stage of a compressor,  $N_s$  simply represents the required speed to give one unit of energy to one unit of air volume while  $D_s$ , reveals the required rotor diameter at each compression stage to give one unit of energy to one unit of air volume.

These parameters are necessary to compare the performance of geometrically different turbomachines with similar  $N_s$  and  $D_s$  or geometrically similar turbomachines with different  $N_s$  and  $D_s$ .

### 3.1. Compressors

Within the compressor chain, the first compressor draws in ambient air from the atmosphere while each subsequent compressor stage takes in air that has been pre-pressurized by the preceding compression stage.

Mass flow rates, compression ratios, and intake temperatures, remain consistent across all compressors; the only distinguishing factor is the intake pressure.

In practice, each compressor within each compression stage may consist of several stages, referred to as  $N_{st}$  in multistage compressors.

This section is dedicated to examining how variations in intake pressure affect the size and cost of different components within the compressors. In this regard, two axial compressors of similar power and compression ratio are considered, each operating with distinct suction pressures. To establish an equivalent performance condition for both compressors, it is necessary for them to share equal values of  $N_s$  and  $D_s$ .

The first compressor,  $Comp_A$ , as shown in Fig. 3, inducts air with pressure  $p_{in,A}$  and temperature  $T_{in}$  and the second compressor,  $Comp_B$



**Table 1**  
The number of compression stages for different storage pressures.

Desired Storage Pressure (bar)	Code	Number of compression stages, $n$	$r_c$ for the last compressor
$p \leq 2.42$	–	1	$p$
$2.42 < p \leq 5.86$	–	2	$\frac{p}{2.42}$
$5.86 < p \leq 14.17$	a	3	$\frac{p}{2.42^2}$
$14.17 < p \leq 34.3$	b	4	$\frac{p}{2.42^3}$
$34.3 < p \leq 83$	c	5	$\frac{p}{2.42^4}$
$83 < p \leq 200.86$	d	6	$\frac{p}{2.42^5}$
$200.86 < p \leq 486$	e	7	$\frac{p}{2.42^6}$

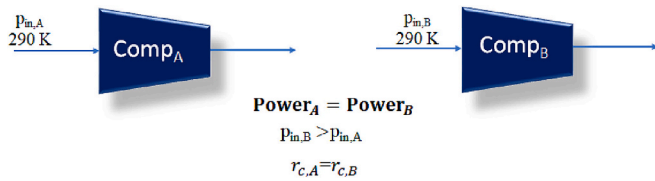


**Fig. 3.** Schematic of the two compared compressors.

intakes air with pressure  $p_{in,B}$  ( $\frac{p_{in,B}}{p_{in,A}} : \Pi > 1$ ).

Assumptions during this analysis are:

- The ideal gas assumption applies to both compressors.
- The compressors absorb the same power.
- The compressors share the same compression ratio.
- The two compressors have similar suction temperatures and consequently similar outlet temperatures.

Based on the above assumptions, the compressors share similar mass flowrates,  $\dot{m}$ . However, the intake volume flow rate,  $\dot{Q}_{in}$  of the  $Comp_B$  would be less than that of  $Comp_A$  because  $Comp_B$  sees higher inlet air density,  $\rho$ .

$$\rho_A \dot{Q}_{in,A} = \rho_B \dot{Q}_{in,B} \quad (5)$$

$$\dot{Q}_{in,B} = \frac{1}{\Pi} \dot{Q}_{in,A} \quad (6)$$

Based on equal specific speed and equal specific diameter for both compressors, which guarantee similar performance, the required rotational speed of  $Comp_B$ ,  $N_B$  should exceed that of  $Comp_A$  by the factor  $\sqrt{\Pi}$ :

$$\frac{N_A Q_A^{0.5}}{(gH)^{0.75}} = \frac{N_B Q_B^{0.5}}{(gH)^{0.75}} \quad (7)$$

$$N_B = \sqrt{\Pi} N_A \quad (8)$$

### 3.1.1. Effects of intake pressure on the size and weight of rotors and blades

Having an equal specific diameter for both examined compressors, A and B, suggests that the rotor diameter of  $Comp_B$  would be smaller than that of  $Comp_A$  by the factor  $\frac{1}{\sqrt{\Pi}}$ :

$$\frac{D_A (gH)^{0.25}}{(Q_A)^{0.5}} = \frac{D_B (gH)^{0.25}}{(Q_B)^{0.5}} \quad (9)$$

$$D_B = \frac{1}{\sqrt{\Pi}} D_A \quad (10)$$

This comparison of rotor diameters remains valid based on the present methodology, applicable to both single-stage and multistage

compressors. In multistage compressors, the initial rotor is the largest, and subsequent rotors decrease in diameter through the compression stages. Comparing the first stage of two multistage compressors—identical in compression ratio, power, and suction temperature but differing only in intake pressure—offers valuable insights into the size relationship between these compressors. This comparison can extend to the subsequent stages as well.

The tip velocity,  $U_t$ , would then be equal for both compressors based on:

$$U_t = N\pi D \quad (11)$$

The compressor rotor diameter can be calculated by [17]:

$$D^2 = \frac{4\dot{m}}{\rho\pi \left[ 1 - \left( \frac{D_h}{D_t} \right)^2 \right] C_x} \quad (12)$$

From Eq. 12, if the hub to tip ratio,  $\frac{D_h}{D_t}$  is constant for both compressors, it can be similarly concluded that higher intake pressures, require a smaller rotor size.

The ideal gas assumption, in conjunction with Eq.10, leads to a conclusion similar to that deduced from Eq.12.

Following the design principles of turbomachinery, the rotor width in  $Comp_B$  would be reduced by almost a similar factor when compared to  $Comp_A$ .

The next component to consider is the blade. Blades are analysed by comparing their volumes as an indicator of size and mass. The volume of each blade can be calculated by [17]:

$$\text{Volume of blade} = K \frac{D_{\text{blade}}^3}{\beta^2} \quad (13)$$

where  $K$  is a constant typically 0.012 for compressors [17]. The blade aspect ratio,  $\beta$ , which is the ratio of the blade chord to the blade height, is commonly in the range of 1 to 1.5.

The number of blades can be then calculated by [17]:

$$\text{Number of blades} = K \frac{\frac{\pi}{2} D_n \text{Solidity}}{\beta h_{\text{blade}}} \quad (14)$$

Blade solidity, also called blade pitch, is the ratio of aerodynamic chord to the distance between two blades. The ideal value of solidity depends on pressure. Higher fluid pressure increases the risk of flow separation and detachment, causing stalls. To prevent this at high pressures, thinner blades with lower solidities are preferred.

Considering the points mentioned previously, the hub diameter and height of the blades for the  $Comp_B$  would be smaller both by the factor  $\frac{1}{\sqrt{\Pi}}$  compared to  $Comp_A$ . The volume of blades and consequently the weight of the blades would decrease in  $Comp_B$  compared to  $Comp_A$  at least by the factor  $\frac{1}{\Pi\sqrt{\Pi}}$ . Considering the  $Comp_B$ , would have fewer blades to ensure smaller solidity and this in turn further reduces the weight.

### 3.1.2. Effects of intake pressure on the size and weight of casing

For an axial compressor with a truncated-cone shape casing, length, thickness, and inlet and outlet diameters can entirely characterize the casing components. The influence of thickness and length on costs are discussed here.

**3.1.2.1. Thickness of the casing.** Two criteria are applied for calculation of the thickness of compressors casings,  $t_{\text{casing}}$  and the greater thickness is ultimately accepted. The first observation calculates the minimum required thickness which can withstand the penetrating kinetic energy of a blade fragment without deformation. Based on which the minimum casing thickness is determined by setting the kinetic and deformation energy equal [18].

$$t_{\text{Casing}} \geq \frac{0.4 \times E_{\text{kin,blade}} \times J}{\sigma_y^2 \times h_{\text{blade}} \times c_{\text{blade}}} \quad (15)$$

The kinetic energy of the blades,  $E_{\text{kin,blade}}$  (J) can be calculated by [18]:

$$E_{\text{kin,bl}} = \left( \frac{1}{8} m_{\text{blade}} D_t^2 \right) N^2 \quad (16)$$

A further criterion for the thickness of the casing ensures that the casing can withstand the maximum air pressure within the compressor. This is satisfied by the following relation, treating the casing as a pressure vessel with a truncated-cone shape with specified maximum and minimum radii, denoted as  $R_{\text{max}}, R_{\text{min}}$ . The maximum air pressure,  $p_{\text{max}}$  within the casing is typically set equal to the discharge pressure [15]:

$$t_{\text{Casing}} \geq \frac{1}{\cos \phi} \frac{R_{\text{max}} p_{\text{max}}}{(S \times E - 0.6 p_{\text{max}})} \quad (17)$$

Based on both constraints, the casing of  $\text{Comp}_B$  would be thicker than that of  $\text{Comp}_A$  by the factor of  $\sqrt{\Pi}$ .

**3.1.2.2. Length of the casing.** The casing length,  $L_C$  is a reliable indicator of the compressor length that can be calculated by [19]:

$$\frac{L_C}{D_M} = 0.2 + \left[ 0.234 - 0.218 \left( \frac{D_h}{D_t} \right)_{\text{inlet}} \right] \times N_{\text{st}} \quad (18)$$

Eq. (18) correlates the ratio of length to the mean diameter,  $D_M$  with the number of stages,  $N_{\text{st}}$  within the casing and the ratio of hub-tip diameter at the inlet. The mean diameter is the average of max and minimum diameter of the truncated-cone casing at both ends of the compressor. Based on the performed analysis, the mean diameter for  $\text{Comp}_B$  is  $\frac{1}{\sqrt{\Pi}}$  of that of  $\text{Comp}_A$ .  $N_{\text{st}}$  is equal for  $\text{Comp}_A$  and  $\text{Comp}_B$  due to their matching compression ratios. As mentioned before, the hub-to-tip radius ratio is set equal for both compressors. Therefore, the length of  $\text{Comp}_B$  would be  $\frac{1}{\sqrt{\Pi}}$  of the length of  $\text{Comp}_A$ .

**3.1.2.3. Mass of the casing.** Based on what has been shown for the length and thickness of the compressor casings A and B, the weight of the casing for  $\text{Comp}_B$  would be  $\frac{1}{\sqrt{\Pi}}$  of that of  $\text{Comp}_A$ .

The calculations for rotor, casing size and weight indicate that the overall size of  $\text{Comp}_B$  with higher suction pressure would be less than that of  $\text{Comp}_A$ . Assuming similar materials are used for both compressors, the reduction in size corresponds to a reduction in weight by a similar factor. This decrease in compressor weight directly results in a lower price for  $\text{Comp}_B$  compared to  $\text{Comp}_A$ .

### 3.1.3. Overall weight of compressors

So far, a first order calculation has been performed to estimate size and weight of the main parts of the compressors like rotors, blades, and casings. Furthermore, there is a correlation reported by NASA [19] for estimation of overall weight of a compressor which can be applied here to make another comparison:

$$W_{\text{Comp}} = K_C D_M^{2.2} N_{\text{st}}^{1.2} \left[ 1 + \frac{\frac{L_C}{D_{M,1}}}{\left( \frac{L_C}{D_{M,1}} \right)_{\text{Ref}}} \right] \quad (19)$$

$\left( \frac{L_C}{D_{M,1}} \right)_{\text{Ref}}$  is a reference length to diameter ratio based on Eq. (18), assuming  $\left( \frac{D_h}{D_t} \right)_{\text{inlet}} = 0.7$  by NASA [19].

$$\left( \frac{L_C}{D_{M,1}} \right)_{\text{Ref}} = 0.2 + 0.081 N_{\text{st}} \quad (20)$$

Taking the previous calculations into Eq. 19 to compare the overall

weight of the compressors,  $\text{Comp}_B$  would be much less heavy having a weight of about  $\frac{1}{\pi}$  of the  $\text{Comp}_A$ .

So far, two different approaches have been introduced to compare the overall weight of compressors. The first scheme compares the weights of major parts of the two compressors, while the second scheme employs the NASA equation to directly compare the overall weight of the compressors. According to the first scheme, all major parts of  $\text{Comp}_B$  including rotor, and casing shrink by a factor of  $\frac{1}{\sqrt{\Pi}}$  compared to  $\text{Comp}_A$ . This reduction in size, assuming the same material for both compressors, serves as an indicator of a similar reduction in weight. However, the second approach reveals a much more significant reduction in weight. The minimum reduction in overall weight, represented by the factor of  $\frac{1}{\sqrt{\Pi}}$  is considered as the benchmark for further analysis.

In summary, Table 2 shows how compressor components alter in size/weight when the suction pressure increases by the factor  $\Pi$ . Because similar turbomachinery guidelines apply to both compressors and expanders, the information presented in Table 2 can also be expanded to encompass expanders.

## 4. Available observations for cost of compressors

Two common approaches for cost estimation are found in the literature. The more popular first approach estimates the cost as a function of the compressor's power. The second approach involves using the size of the compressor and comparing it with a benchmark compressor to estimate the cost. Both methods are subsequently discussed in detail in Sections 4.1 and 4.2.

### 4.1. Cost as a function of power

In the existing literature, several correlations can be found to estimate the cost of compressors, among those what proposed by Gabrielli, and Singh [20] and Douglas [21] (following equations respectively) are more popular.

$$\text{Cost}_{\text{comp}} (\$) = \frac{100}{1 - \eta_{\text{isen}}} \dot{m}_{\text{air}} r_c \ln(r_c) \quad (23)$$

$$\text{Cost}_{\text{comp}} (\$) = 5840 (\text{Power}(\text{kW}))^{0.82} \quad (24)$$

Most of available correlations for cost estimation have a primary focus on power consumption as the pivotal factor influencing the cost.

The correlation by Gabrielli and Singh [20], Eq. 23 can be rewritten like:

$$\text{Cost}_{\text{comp}} (\$) = \frac{100}{1 - \eta_{\text{isen}}} \frac{r_c}{RT_{\text{in}}} \text{Power} \quad (27)$$

Eq. 27 reveals that Gabrielli and Singh, approximate the cost of compressor as a function of its power, and its inlet air intake temperature,  $T_{\text{in}}$ . Both factors were similar for the considered compressors A and B in this study and based on Gabrielli and Singh viewpoint both compressors should have similar price despite the demonstrated significant difference between their size.

The correlation presented by Douglas (Eq. 24) asserts that compressors with equal powers would also have the same cost. Based on such a viewpoint both examined compressors A, and B would have similar costs despite the demonstrated significant difference between their size. This contradicts what was demonstrated in earlier sections, where it was established that power alone is not the sole factor influencing compressor cost, with suction pressure also playing a significant role.

On the other hand, it can be demonstrated that the cost per unit of power decreases with an increase in power. This aspect has been considered in the proposed correlation by Douglas [21] (Eq. 23) but has been overlooked in Gabrielli and Singh's correlation [20].

**Table 2**Effects of increased intake pressure (increase by factor of  $\Pi$ ) on various aspects of compressors/turbines.

Intake pressure	Blades weight	Rotor diameter	Rotational speed	Thickness of casing	Length of casing	Weight of casing	Overall weight
$\times \Pi$	$\times \frac{1}{\Pi\sqrt{\Pi}}$	$\times \frac{1}{\sqrt{\Pi}}$	$\times \sqrt{\Pi}$	$\times \sqrt{\Pi}$	$\times \frac{1}{\sqrt{\Pi}}$	$\times \frac{1}{\sqrt{\Pi}}$	$\times \frac{1}{\sqrt{\Pi}}$

#### 4.2. Cost as a function of size

The ‘‘Rule-of-Thumb’’ [22] serves as a practical approach to establish a connection between changes in cost and variations in size. Based on this rule, costs are usually correlated in terms of a base cost multiplied by a ratio of sizes raised to the power ‘‘ $n$ ’’.

$$\text{Cost}_2 = \text{Cost}_{\text{ref}} \left( \frac{\text{size}_2}{\text{size}_{\text{ref}}} \right)^n \quad (21)$$

where  $n$  depends based on the type of the equipment. The size should be a ‘‘cost dependent’’ parameter like casing mean diameter or length. For the axial compressors,  $n$  is suggested to be 1.33 for the range of 4000–20,000 kW, and to be 0.9 for the range of 30–300 kW [22].

### 5. A comprehensive model for compressors cost

#### 5.1. Effects of power and pressure

Power and size are the only two parameters that have been individually considered as influential parameters on the cost of compressors in the available literature. However, the most influential factor, intake pressure, along with several other factors, has been overlooked.

In this section, a comprehensive model for estimating the cost of compressors is presented. This model integrates the relationship between the overall size and the suction pressure of the compressors, which was previously discussed in the preceding section, with the Rule of Thumb for adjusting the power-related cost correlations found in the literature.

In summary, it was determined that when the suction pressure enhances by the factor  $\Pi$  the overall size reduces by the factor  $\frac{1}{\sqrt{\Pi}}$ . Based on the Rule of Thumb, the cost of a compressor which intake air with pressures  $\Pi$  times ambient pressure, will be decreased by  $\left(\frac{1}{\sqrt{\Pi}}\right)^n$  in comparison with a similar compressor which intakes air at ambient pressure.

#### 5.2. Other aspects

Capital Cost provision for any machinery involves considering several influencing factors like technology improvement, inflation, market demand, and cost of manufacturing.

Advancing technology lowers future machinery costs by improving efficiency, materials, and design while reducing labour expenses through automation and advanced manufacturing. To consider effects of technology improvement on the cost of machinery the variation of machinery costs over years would be a useful clue [23,24]. Schmidt et al. [23], determined the lifetime cost of 9 electricity storage technologies in 12 power system applications from 2015 to 2050 including CAES. Unlike some battery storage technologies, they claimed that the overall cost of CAES would remain unchanged in comparison with that of 2015 until 2030 and may have 2 % increase from 2030 to 2050. With an average cost increase of 3.5 % attributed to land and plant fields (specifically for the UK), the machinery cost must potentially experience a similar 3.5 % reduction over time, to satisfy Schmidt's theory. Baxter [24], on the other hand, anticipates a machinery cost reduction of 4–4.5 % between 2020 and 2050.

Any cost provision should account for the potential increase in prices of raw material, labour and other expenses due to inflation. Because

manufacturing costs are typically expressed per ton of material, the impact of inflation, which raises material costs, might not appear to significantly affect the overall machinery cost over time.

The existing correlations for cost approximation have certainly been derived through curve-fitting using various available data. Their applicability could be enhanced by implementing certain adjustments to consider the effects of suction pressure and technological advancements. Using these along with some recent economic data shown in Table 3 as well as the above performed analysis, and the Rule of Thumb altogether, a correlation for estimation of compressors cost is proposed to integrate effects of intake pressure, power, and technology level:

$$\text{Cost}_{\text{comp}} (\$) = \left( \frac{1}{\sqrt{P_{\text{Inlet}}}} \right)^n \frac{1}{(1 + r_t)^{\text{year}-2023}} \left[ \frac{300}{1 - \eta_{\text{isen}}} (\text{power}(kW))^{0.68} \right] \quad (22)$$

where,  $P_{\text{Inlet}}$  is the intake pressure in bar,  $\eta_{\text{isen}}$  represents the isentropic efficiency of the compressor;  $r_t$  denotes the rate of technology improvement. For the case of PCS machinery  $r_t$  is considered to be around 0.002 [23,24]. The term,  $\left(\frac{1}{\sqrt{P_{\text{Inlet}}}}\right)$ , in the above equation, accounts for size reduction due to accounting effects of inlet pressure based on the performed analysis; According to the Rule of Thumb,  $n = 1.33$  for axial compressors.

The deviation of the proposed correlation from the available economic data are shown in the 7th row of the Table 3.

### 6. Expanders

The observations made regarding the impact of pressure on compressor size and weight can also be extended to expanders, given that both are classified as turbomachinery. Consequently, individual calculations for expanders would not be required in this study. Based on the prior analysis, a turbine operating with a higher intake pressure would exhibit reduced dimensions and weight in comparison to a turbine with lower intake pressure. This implies that in a multi-stage expansion setup with expanders sharing similar expansion ratios, the initial expander—having the highest inlet pressure—would be more cost-effective than subsequent expanders with lower inlet pressures.

Similar to what was discussed for compressors, the size change due to intake pressure of an expander can be related to its cost variation by the Rule of Thumb, Eq. 21. The corresponding factor  $n$  is suggested to be 0.8 for the gas driven turbines/expanders.

One of the most popular correlations for estimating cost of expanders is proposed by Roosen et al. [28]. Other available equations follow the same format with only slight variations in the constant factors [10,20].

$$\text{Cost}_{\text{Expander}} = \frac{1148}{1 - \eta_{\text{isen}}} \ln \left( \frac{P_{\text{in}}}{P_{\text{out}}} \right) \{ 1 + \exp[0.036T_{\text{in,Ex}} - 65.66] \} \quad (23)$$

where,  $\eta_{\text{isen}}$  represents the isentropic efficiency of the expander;  $T_{\text{in,Ex}}$  denotes the gas inlet temperature to the expander (K), and  $\left(\frac{P_{\text{in}}}{P_{\text{out}}}\right)$  represents expansion ratio. Considering the time value of money along with considering effects of inlet pressure on the expander costs, as well as real economic data collected from some established plants shown in Table 3, the following correlation is put forth to calculate cost of each turbine in a multi-stage expansion process with similar expansion ratio across the stages:

**Table 3.**  
Reported costs of compressors/turbines for some executed plants.<sup>a</sup>

	Black and Veatch*, 2010 [25]	McIntosh <sup>†</sup> , 1991 [24]	Siemens <sup>‡</sup> [26]	Siemens [26]	Siemens [26]	Ireland <sup>§</sup> [27]	Huntorf <sup>¶</sup> [24]
Power (MW)	262	110	115	115	115	140	290
Duration, hours	15	26	10	20	30	10.5 (charging) 5 (discharging)	8 (charging) 2 (discharging)
Reported compressors cost \$/kW	158	520 (compressors + turbines)	197	219	241	210	320
Reported Turbines cost \$/kW	327		309	344	378	249 (A-CAES) 358 (D-CAES)	222 (A-CAES) 320 (D-CAES)
Calculated compressor cost based on the proposed correlation in this study	161	234	189	196	213	208	291
Calculated turbine cost based on the proposed correlation in this study	331	330	326	331	332	462	511
Relative Dev (%)	2 %	8 %	4 %	10 %	11 %	1 %	9 %

<sup>a</sup> It is worth noting that except for Huntorf and McIntosh plants, Table 3 data do not refer to existing established plants. Moreover, the cost reported in this table are not real cost, but estimated cost.

<sup>\*</sup> In 2009, Black & Veatch entered into a contract with the National Renewable Energy Laboratory to provide cost and performance estimates for power-generating technology. These estimates were synthesized from various sources in late 2009 and early 2010. A confidential in-house CAES reference study from an independent power producer served as the foundation for the specific estimate, with the range derived from historical data. The estimate assumed a two-unit recuperated expander with storage within a solution-mined salt dome, providing approximately 262 MW net power with 15 h of storage. The configuration included five compressors, and the capital cost, estimated at \$900/kW in 2010, accounted for a range of  $-30\%$  to  $+75\%$ . No cost improvement was projected over time.

<sup>†</sup> There are only two CAES plants currently in operation internationally: the 290 MW plant in Huntorf, Germany, and the 110 MW McIntosh Plant in Alabama, USA. Deployed in 1991, the McIntosh Plant had an installation cost of \$591/kW, equivalent to \$1068/kW in 2020 USD. It's important to note that external funding was utilized, potentially resulting in a higher actual cost. Factoring in improvements to the powertrain's performance, the total installed cost reaches \$1200/kW. This figure encompasses additional permitting requirements beyond 1991 regulations, and the implementation of selective catalyst reduction for nitrogen oxide incurs an extra cost of \$90/kW in 2020 USD (HDR Inc., 2014). The McIntosh plant, with cavern capacity of about 538,000 m<sup>3</sup> uses three compressors and two expanders to provide pressures between 46 and 75 bars.

<sup>‡</sup> Siemens provided cost metrics for a CAES plant with numbers on the low end of the range investigated that were interpreted as future target costs. The cavern capacity of 800,000 m<sup>3</sup> is considered. Authors were unable to find additional details. Therefore, similar compressors and expanders with ratios as those considered in this study (2.42) are considered for this case for estimating the cost.

<sup>§</sup> A CAES facility utilizing cavern storage excavated from the salt beds in County Antrim, located in the northeast of Ireland. This research has formulated intricate technical cost models specific to CAES systems. These models are informed by cavern design details and project parameters obtained from the project storage platform for the integration of renewable energy. The compression units consist of three-stage electrically-driven compressors powered by grid electricity, while the expansion unit features two expanders. Each stage in the multi-stage compression assumes an equal pressure ratio. The compressors are estimated to consume approximately 100 MWe per unit for the given duty. The cavern's net available volume for compressed air storage is 300,000 m<sup>3</sup>, with a pressure range of 50 to 70 bar, resulting in a storage capacity of 6590 t of stored air. The CAES air turbine operates at a constant inlet pressure of 45 bar. Polytropic efficiencies for both expanders/turbines and compressors are assumed to be 85 %, with electric motor and generator efficiencies assumed at 98 %.

<sup>¶</sup> The first large CAES plant, the Huntorf power plant, was set up in Germany in 1978. It uses two salt domes for storage and operates daily, charging with compressed air for 8 h and running for 2 h at a 290 MW power rating. Using a 2-stage air-compression/expansion system, the Huntorf plant operates at a pressure range of 46–72 bars with an efficiency of 42 % and cavern capacity of about 310,000 m<sup>3</sup>. The data reported by [24] is in the order of  $+30\%$ ,  $-30\%$ .

$$\frac{Cost_{Expander}|_{stage,i}}{Cost_{Expander}|_{First\ stage}} = \left(\sqrt{\Pi}\right)^{(i-1)^n} \quad (24)$$

The exergy of the thermal energy (reheating among the expansion stages),  $EX|_{Reheating}$  which cause the temperature raise up to  $T_H$ , can be calculated by:

$$Cost_{Expander}|_{First\ stage} = \frac{1}{(1+r_t)^{year-2023}} \left[ \frac{1800}{1-\eta_{isen}} \dot{m}_{air} \ln\left(\frac{p_{in}}{p_{out}}\right) \{1 + \exp[0.036T_{in,Ex} - 65.66]\} \right] \quad (25)$$

In a multi-stage expansion process with similar expansion ratio between the stages, the cost of turbines increases across the stages by the factor  $\sqrt[n]{Expansion\ ratio}$  if the intake gas temperature for all turbines is set similar, where  $n$  is set 0.8 based on the Rule of Thumb.

### 6.1. Number of expansion stages

The number of expanders is set equal to the number of compressors, ensuring a similar configuration of heat exchangers in the expansion unit as in the compression unit. The heat recovered from the inter-cooling stages of the compressors is directly transferred to the air entering the corresponding expansion stages, resulting in similar inlet and outlet temperatures for the expanders as for the compressors.

$$EX|_{Reheating} = Q \left[ 1 - \frac{T_{ref}}{T_H - T_{ref}} \ln\left(\frac{T_H}{T_{ref}}\right) \right] \quad (26)$$

## 7. Results and discussion

The primary objective of this study is to assess the effect of operating pressure on the cost of the PCS machinery in AA-CAES applications. In this study, various storage pressures are achieved by utilizing predefined compressors with a compression ratio of 2.42. This implies the use of different stages of compression.

For all of the considered final storage pressures, with similar charging or similar discharging time, the mass flowrate of the air is



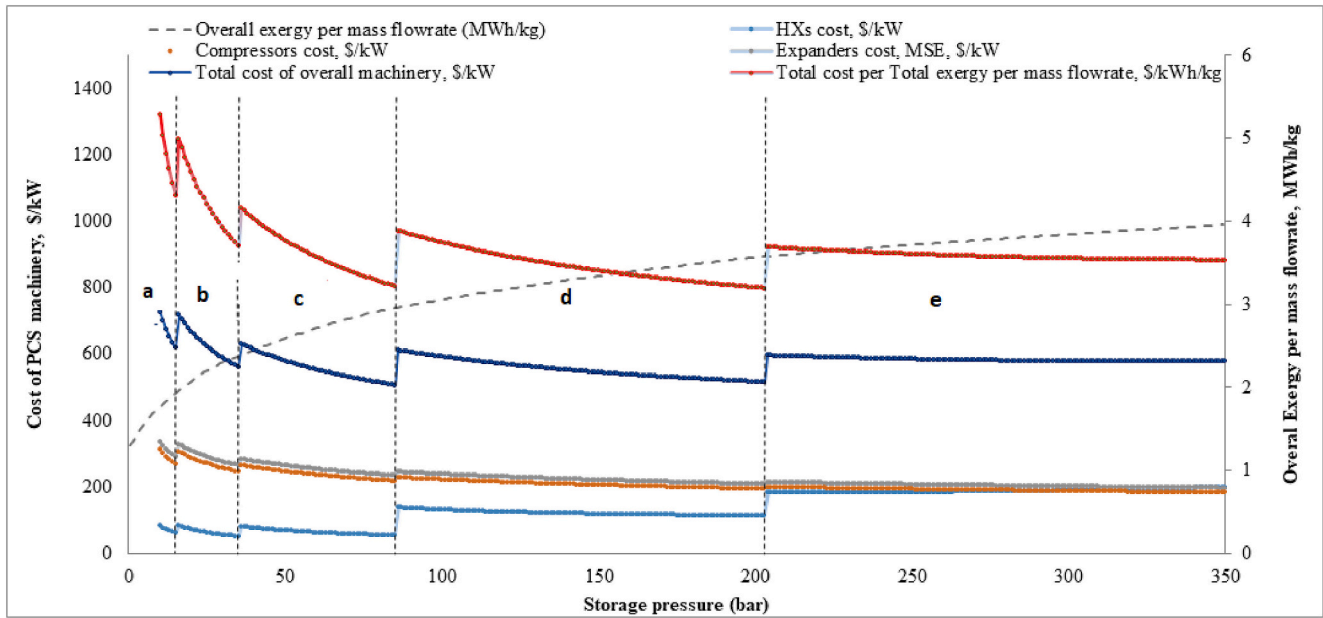


Fig. 4. Cost of PCS machinery vs storage pressure \$/kW.

assumed to be constant. As an example, the compression and expansion stages of a sample 4-stage AA-CAES are shown respectively in Fig. 2. This figure is just an example of several simulated AA-CAES plants in this study.

Taking into consideration that the higher intake pressure machinery is cheaper than lower intake pressure ones as discussed before, the cost of total machinery declines through the compression stages. These are shown in Fig. 4. There are two important remarks in this figure: the first one is about the number of stages that is categorized by a, b, ... e in the figure and the second one about the storage pressure shown in the horizontal axis. The storage pressure indicated on the horizontal axis corresponds to the ultimate pressure that the storage tank of the plant is designed to reach. To achieve this desired storage pressure, which spans from 10 bar to 350 bar in this study, a varying number of compression stages becomes necessary (detailed in Table 1).

In this figure total cost of machinery containing compressors, expanders, and heat exchangers are reported per power of each machine. The cost calculation details regarding the heat exchangers are comprehensively presented in the part II of this paper.

As can be seen in the figure the cost of machinery reduces by increasing the storage pressure. The cost reduction for the lower pressures is more significant while for very high storage pressures as can be seen at the end of the plot, the cost of the machinery hardly varies with pressure. Based on the assessment, the initial compression stage is the most expensive, with costs decreasing as pressure rises. Equipment in later stages is progressively more cost-effective.

The total cost per total exergy of the system declines by pressure as shown in Fig. 4. As the storage pressure increases the slope of the curve reduces since the exergy at the denominator (the dashed grey line) is increasing more than decreasing the cost with the storage pressure. This provides the economic justification of establishing CAES plants with the highest possible storage pressures.

The contribution of each machine can also be observed in Fig. 4. Compressors and expanders tend to be more economical at higher storage pressures.

The cost contribution of each machine at different storage pressures is depicted in Fig. 5. The contribution of compressor and expander costs remains very similar across all the considered storage pressures. For storage pressures below 70 bar, the combined cost of compressors and expanders constitutes approximately 90 % of the total PCS cost. As

storage pressure increases, involving the addition of more compression or expansion stages, the number of compressors and expanders also increases. However, the overall contribution decreases because compressors and expanders at higher operating pressures are more cost-effective than those at lower operating pressures. On the other hand, at higher pressures, heat exchangers contribute to a higher portion of the total cost. Part II will demonstrate how the contribution of heat exchangers' costs increases for higher operating pressures.

As evident from the figure, compressors constitute approximately 43 % of the total machinery cost at 30 bar, whereas in a storage plant with a 350 bar storage pressure, they account for around 31 % of the total cost. The contribution of expander costs varies within the range of 47 % to 34 % of the total cost for storage pressures between 30 and 350 bar. Interestingly, the cost contribution of heat exchangers<sup>2</sup> experiences an increase from 10 % at a storage pressure of 30 bar to about 35 % for a storage pressure of 350 bar.

The other parameter that has been considered is the overall efficiency of the AA-CAES plant which is simply defined by:

$$\eta = \frac{\text{Total Exergy}}{\text{Total isentropic work of compressors}} \quad (27)$$

Fig. 6 shows the overall efficiency for different storage pressures. The overall exergy is the sum of exergy due to all reheating stages (thermal exergy, Eq.26) and the exergy of the pressurized air (mechanical exergy, Eq.2). It is worth noting that the maximum achievable efficiency, reported in the literature to be around 80 % for AA-CAES, occurs at pressures higher than 100 bar and slightly increases for even higher storage pressures.

## 8. Uncertainties

Variations in storage pressure can influence the energy consumption capacity, encompassing changes in the efficiency of power conversion machinery, alterations in energy losses, and potential fluctuations in overall energy consumption. Adjusting the operating pressure may impact the performance and efficiency of the system, affecting how

<sup>2</sup> Detailed cost calculation for heat exchangers is provided in the Part II of this paper.

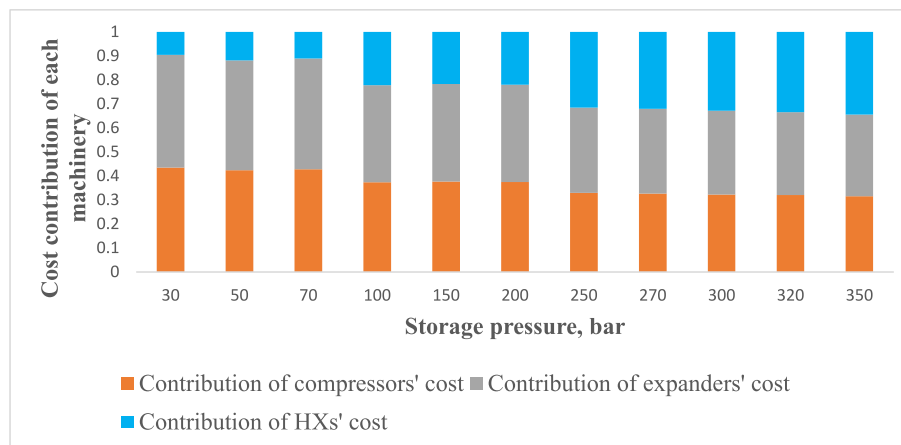


Fig. 5. The cost contribution of each machine at different storage pressures.

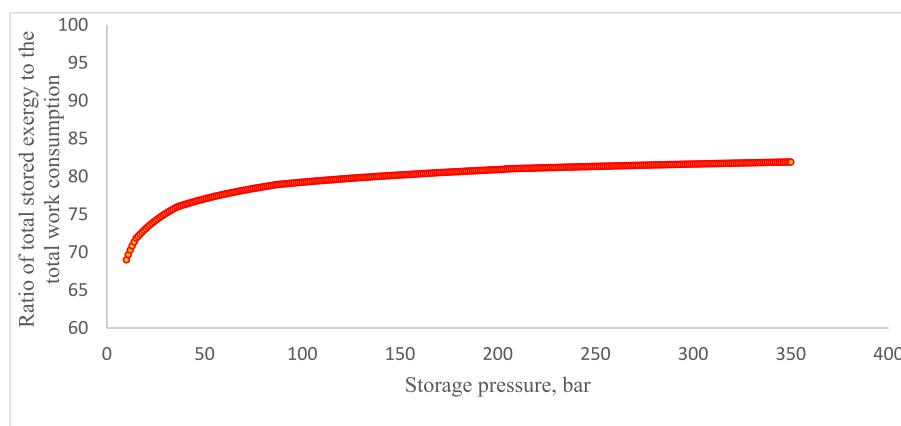


Fig. 6. Overall efficiency vs storage pressure.

much energy is consumed during operations. This is a key consideration in understanding the overall dynamics of an energy storage system under different pressure conditions.

Higher operating pressures may lead to improved efficiency in power conversion machinery, as compressors and expanders may operate more effectively under increased pressure conditions. This can result in a more efficient conversion of compressed air to electricity [29].

Higher pressure conditions might contribute to reduced energy losses during the compression and expansion processes. However, it's essential to assess the entire system design and components to understand how changes in pressure impact energy losses [29].

The overall energy consumption may increase with higher pressure due to the additional energy required for compression. However, advancements in technology and system design could mitigate this increase, and the relationship between pressure and energy consumption may not be linear.

Increasing storage pressure can positively influence exergy. Studies suggest that higher storage pressures lead to reduced exergy losses, enhancing overall system efficiency and performance [30,31].

Increasing storage pressure tends to reduce uncertainties in system costs. Studies demonstrate that higher pressures can enhance round-trip efficiency and exergy efficiency, contributing to more predictable cost estimations [31]. Higher storage pressures generally lead to improved energy storage capacity. As the storage pressure increases, the amount of energy stored also increases, contributing to a more predictable and efficient energy consumption capacity [32].

## 9. Conclusion

The present study thoroughly investigates the effects of operating pressure on the components size, overall sizes, and subsequently the costs of PCS machinery with application in AA-CAES plant. Both compressors and expanders, falling under the turbomachinery classification, were examined. A comprehensive investigation has been conducted for the heat exchangers and is presented in part II of this paper. The analyses for both turbomachines and HXs were conducted with the objective of integrating the impacts of intake pressure on the size of key components for each machine. The cost variations of each machine were then approximated based on the alterations in size. In existing literature, common approaches estimate costs based on power or size, overlooking the impact of intake pressure. Our findings highlight that suction pressure plays a significant role in influencing compressor/expander costs, a factor frequently neglected in current methodologies. The analysis in this study employed a conceptual engineering approach, leading to specific adjustments in the available correlations for the cost of compressors and expanders to account for the influences of suction pressure and technological advancements.

- Based on the obtained data, contrary to common perception, increasing the number of compression stages to achieve higher storage pressures not only doesn't lead to a linear increase in capital costs per power but also results in a decrease in costs per power.
- The PCS machinery cost for an AA-CAES plant with a storage pressure of 350 bar is \$580/kW, offering 3.96 MWh/kg overall exergy per mass flowrate. In comparison, the cost for a storage pressure of

90 bar is \$605/kW, providing 2.94 MWh/kg overall exergy per mass flowrate.

- To establish an AA-CAES plant with storage pressure 200 bar instead of 50 bar with the same mass flowrate, there is a potential for a 7.8 % reduction in \$/kW expenditure to achieve 44 % more exergy (MWh/kg). For another comparison, an AA-CAES plant with a storage pressure of 350 bar costs 1.5 % less, while providing around 11 % more exergy compared to a storage pressure of 205 bar.
- The overall costs of expanders and compressors for the AA-CAES case with a 350-bar storage pressure are \$196/kW and \$183/kW, respectively. In comparison, for a storage pressure of 90 bar, the costs are \$244/kW and \$227/kW for expanders and compressors, respectively.
- The contributions of compressors and expanders to the overall machinery costs decrease with an increase in storage pressure. For instance, considering compressors, the cost contribution decreases from 43 % of the total machinery cost at 30 bar to around 31 % at 350 bar. A similar trend is observed for expanders, where the cost contribution varies from 47 % to 34 %. Conversely, the cost contribution of heat exchangers (HXs) increases from 10 % at a storage pressure of 30 bar to approximately 35 % for a storage pressure of 350 bar.

Looking forward, numerous avenues for future research emerge from the insights gained in this study. Future studies may explore optimizing strategies for cost-effective storage pressure, taking into account dynamic operational costs and the long-term economic viability of AA-CAES plants. Considering the storage containment in the costs adds significant value to advancing this work as it is not, of course, sufficient to focus only on the power-conversion equipment in an energy storage system and one must also consider the cost and viability of the actual resources used to store energy. Moreover, the study's conceptual engineering approach has set the stage for refining cost correlations in compressors and expanders, considering suction pressure influence. Future research could build upon these adjustments, refining cost estimation models for turbomachinery.

#### Authors statement

The authors wish to acknowledge the generous support received from the United Kingdom's Engineering and Physical Sciences Research Council (EPSRC) for the completion of this work. The research presented in this paper was made possible through the research grant titled 'Sustainable, Affordable and Viable Compressed Air Energy Storage' (EP/W027569/1), provided by EPSRC.

We affirm that there are no conflicts of interest to disclose, and the research was conducted in compliance with ethical standards. All authors have made substantial contributions to the conception, design, analysis, and interpretation of data, and have been actively involved in drafting and revising the manuscript.

#### CRedit authorship contribution statement

**Zahra Baniamerian:** Writing – original draft, Validation, Software, Resources, Methodology, Investigation, Formal analysis, Data curation, Conceptualization. **Seamus Garvey:** Writing – review & editing, Supervision, Project administration, Funding acquisition, Conceptualization. **James Rouse:** Writing – review & editing, Supervision. **Bruno Cárdenas:** Writing – review & editing, Methodology, Investigation. **Daniel L. Pottie:** Writing – review & editing, Methodology. **Edward R. Barbour:** Writing – review & editing, Funding acquisition. **Audrius Bagdanavicius:** Writing – review & editing, Funding acquisition.

#### Declaration of competing interest

The authors declare that they have no known competing financial

interests or personal relationships that could have appeared to influence the work reported in this paper.

#### Data availability

Data will be made available on request.

#### Acknowledgement

The authors would like to thank the United Kingdom's Engineering and Physical Sciences Research Council (EPSRC) for supporting this work through the following research grant: 'Sustainable, Affordable and Viable Compressed Air Energy Storage' (EP/W027569/1). The authors would also like to express their gratitude to the reviewers who contributed to improving the quality of this paper.

#### References

- [1] M. Cheayb, M.M. Gallego, M. Tazerout, S. Poncet, A techno-economic analysis of small-scale trigenerative compressed air energy storage system, *Energy*, volume 239, Part A 15 (January) (2022) 121842.
- [2] M.C. Bushehri, S.M. Zolfaghari, M. Soltani, M.H. Nabat, J. Nathwani, A comprehensive study of a green hybrid multi-generation compressed air energy storage (CAES) system for sustainable cities: Energy, exergy, economic, exergoeconomic, and advanced exergy analysis, *Sustain. Cities Soc.* 101 (February) (2024) 105078.
- [3] R. Cao, W. Li, X. Cong, Y. Duan, Energy, exergy and economic (3E) analysis and multi-objective optimization of a combined cycle power system integrating compressed air energy storage and high-temperature thermal energy storage, *Appl. Therm. Eng.* 238 (1 February) (2024) 122077.
- [4] M. Mersch, P. Sapin, A.V. Olympios, Y. Ding, N.M. Dowell, C.N. Markides, A unified framework for the thermo-economic optimisation of compressed-air energy storage systems with solid and liquid thermal stores, *Energy Convers. Manag.* 287 (1 July) (2023) 117061.
- [5] E.H. Gülleryüz, D.N. Özen, Advanced exergy and exergo-economic analyses of an advanced adiabatic compressed air energy storage system, *Journal of Energy Storage*, Part D 55 (30 November) (2022) 105845.
- [6] P. Zhao, Y. Dai, J. Wang, Design and thermodynamic analysis of a hybrid energy storage system based on A-CAES (adiabatic compressed air energy storage) and FESS (flywheel energy storage system) for wind power application, *Energy* 70 (2014) 674–684.
- [7] C.R. Matos, P.P. Silva, J.F. Carneiro, Economic assessment for compressed air energy storage business model alternatives, *Appl. Energy* 329 (2023) 120273.
- [8] R. Madlener, J. Latz, Economics of centralized and decentralized compressed air energy storage for enhanced grid integration of wind power, *Appl. Energy* 101 (2013) 299–309.
- [9] E. Bozzolani, Techno-Economic Analysis of Compressed Air Energy Storage Systems, MSc Thesis, CRANFIELD UNIVERSITY, 2010.
- [10] B. Zakeri, S. Syri, Electrical energy storage systems: a comparative life cycle cost analysis, *Renew. Sust. Energ. Rev.* 42 (2015) 569–596.
- [11] H. Chen, H. Wang, R. Li, H. Sun, Y. Zhang, L. Ling, Thermo-dynamic and economic analysis of a novel pumped hydro-compressed air energy storage system combined with compressed air energy storage system as a spray system, *Energy* 280 (1 October) (2023) 128134.
- [12] E. Assareh, A. Ghafouri, An innovative compressed air energy storage (CAES) using hydrogen energy integrated with geothermal and solar energy technologies: a comprehensive techno-economic analysis - different climate areas- using artificial intelligent (AI), *Int. J. Hydrog. Energy* 48 (34, 22 April) (2023) 12600–12621.
- [13] S.M. Alirahmi, A. Raisi, B. Ghasemi, A.A. Nadooshan, Comprehensive techno-economic assessment and tri-objective optimization of an innovative integration of compressed air energy storage system and solid oxide fuel cell, *Renew. Energy* 218 (December) (2023) 119290.
- [14] American Petroleum Institute. API 617: Axial and Centrifugal Compressors and Expander-compressors (8th ed.).
- [15] Fundamentals of Turbomachinery, William W. Peng, ISBN: 978-0-470-12422-2, 2007.
- [16] A method to estimate weight and dimensions of aircraft gas turbine engines Method of analysis, May, 1, NASA report CR 135 170, 1977.
- [17] S. Bretschneider, F. Rothe, M.G. Rose, S. Staudacher, Compressor, casing preliminary design based on features, in: Proceedings of ASME Turbo, Expo 5, ASME, 2008, pp. 1–9.
- [18] David A. Sagerser, Seymour Lieblein, Richard R. Krebs, Empirical expressions for estimation length and weight of axial-flow components of VTOL power plants, NASA technical memorandum, NASA TMX 2406.
- [19] R. Gabbriellini, R. Singh, Economic and scenario analyses of new gas turbine combined cycles with no emissions of carbon dioxide, *J. Eng. Gas Turbines Power* 127 (July) (2005).
- [20] J.M. Douglas, *Conceptual Design of Chemical Processes*, McGraw-Hill, 1988.
- [21] R. Donald, Woods, *Rules of Thumb in Engineering Practice*, First edition, WILEY-VCH Verlag GmbH & Co. KGaA, 2007.

- [22] Oliver Schmidt, Sylvain Melchior, Adam Hawkes, Iain Staffell, Projecting the future levelized cost of electricity storage technologies, *Joule* 3 (2019) 81–100.
- [23] Richard Baxter, Energy storage pricing survey, SANDIA REPORT SAND2021-14700 Printed (November 2021) (2020).
- [24] Black & Veatch, Cost and Performance Data for Power Generation Technologies, Retrieved from Kansas, USA: <https://refman.energytransitionmodel.com/publications/1921/>, 2012.
- [25] Siemens Energy, Roundtrip Efficiency Characterization for Dresser-Rand SMARTCAES Compressed Air Energy Storage Systems. Presentation, Siemens Energy, Munich, Germany, 2018.
- [26] Y. Huang, P. Keatley, H.S. Chen, X.J. Zhang, A. Rolfe, N.J. Hewitt, Techno-economic study of compressed air energy storage systems for the grid integration of wind power, *Int. J. Energy Res.* 42 (2018) 559–569.
- [27] P. Roosen, S. Uhlenbruck, L.K. Pareto, Optimization of a combined cycle power system as a decision support tool for trading off investment vs. operating costs, *Int. J. Therm. Sci.* 42 (2003) 553–560.
- [28] D. An, Y. Li, X. Lin, S. Teng, Analysis of compression/expansion stage on compressed air energy storage cogeneration system, *Front. Energy Res.* 19 September (2023).
- [29] L. Huang, H. Guo, Y. Xu, X. Zhou, H. Chen, Influence of design point on off-design and cycling performance of compressed air energy storage systems-from key processes to the whole system, *Journal of Energy Storage* 57 (January) (2023) 106181.
- [30] X. Xue, J. Li, J. Liu, Y. Wu, H. Chen, G. Xu, T. Liu, Performance evaluation of a conceptual compressed air energy storage system coupled with a biomass integrated gasification combined cycle, *Energy* 247 (15 May) (2022) 123442.
- [31] H. Mozayeni, M. Negnevitsky, X. Wang, F. Cao, X. Peng, Performance study of an advanced adiabatic compressed air energy storage system, *Energy Procedia* 110 (2017) 71–76.
- [32] E. Bazdar, F. Nasiri, F. Haghghat, Optimal planning and configuration of adiabatic-compressed air energy storage for urban buildings application: techno-economic and environmental assessment, *Journal of Energy Storage* 76 (15 January) (2024) 109720.